Supplemental Materials

Flt3Cre+ Kras$^{G12D/+}$ mice develop a transplantable JMML-like myeloid disease

Stefan P. Tarnawsky[1], Rebecca J. Chan[2,3*], Mervin C. Yoder[1,2*]

1. Department of Biochemistry and Molecular Biology, Indiana University School of Medicine, Indianapolis, IN, USA.
2. Department of Pediatrics, Herman B. Wells Center for Pediatric Research, Indiana University School of Medicine, Indianapolis, IN, USA.
3. Department of Medical & Molecular Genetics, Indiana University School of Medicine, Indianapolis, IN, USA.

* Co-Senior Authors

Correspondence

Rebecca J. Chan, 1044 W. Walnut Street, R4-170, Indianapolis, Indiana 46202, USA. Phone: 317.274.4719; E-mail: rchan@iupui.edu.

Methods

Mice
Lox-STOP-Lox $Kras^{G12D/+}$ (1) were purchased from the Jackson Laboratory (Stock #008179) and mated with Flt3Cre+;$ROSA^{mTmG/mTmG}$ mice (2-4) (a kind gift from Dr. Slava Epelman, University of Toronto). All mice were on a C57B6 background. BoyJ mice were bred in-house. All Flt3Cre+ mice were male. Mice were genotyped using polymerase chain reaction protocols (1, 2). Animal studies were approved by the IACUC at the Indiana University School of Medicine.

Timed Matings
In the evening one or two female mice (8-26 weeks of age) were placed in a cage with one male (10-26 weeks of age). The following morning, successful matings were confirmed by visual inspection of a vaginal plug and assigned a gestational age of E0.5.

Transplantations
Lethally irradiated (950cGy) 8-12 week-old female BoyJ animals were used for all transplant experiments. $2x10^6$ fetal liver cells were injected via tail vein. For secondary transplantations $4x10^6$ BM cells were injected.

Peripheral blood analysis
Blood was collected into EDTA-coated tubes and analyzed using the Element HT5 Hematology Analyzer (Heska). Peripheral blood smears were stained using Modified Wright's stain (Fisher).

Cell isolation
Bone marrow cells were flushed from forelimb and hindlimbs. Spleens, thymuses, and livers were triturated with glass cover slides. Enucleated RBCs were depleted using density gradient centrifugation (Sigma #10771) or RBC lysis buffer (Qiagen #158904).

Flow cytometry
Cells were stained at a concentration of 10^7/ml in PBS +2% FBS + 2mM EDTA. Antibodies used are listed in Table S1. Lineage panel= CD3, CD4, CD8, CD11b, CD11c, Gr1, B220, Ter119. Samples were analyzed using the BD SORP-LSRFortessa or BD FACSCANTO II. Samples were sorted using a BD FACSAria. Post run analysis was performed using FlowJo (Treestar). For cell cycle analysis, surface-stained cells were fixed in 1% PFA (Fisher #50-980-487) followed by permeabilization (Fisher 88-8824-00) according to kit instructions.

qPCR
Genomic DNA was isolated from 200-5000 sorted cells using the Qiagen DNeasy Blood & Tissue Kit (#69504). Samples were prepared using FastStart Universal SYBR Green Master (Roche # 04913850001) and were run on a 7500 Real-Time PCR System (Applied Biosystems). Primer sequences are listed in Table S2 below.

Cell culture
BM cells were cultured in IMDM (Fisher #12440079), 10% FBS (Fisher #SH30070.03), and 100 U/ml Penicillin/Streptomycin (Fisher #15140122) supplemented with 440nM β-Mercaptoethanol (Sigma #M6250) and 2mM L-Glutamine (Fisher # 25030-081).

Methylcellulose progenitor assays
Methylcellulose colony formation have been described previously (5). $5x10^4$ BM mononuclear cells were plated in 1ml of methylcellulose medium supplemented with 30% FBS, 2.2% Pen/Strep, 1.2mM L-Glutamine, and 440nM β-Mercaptoethanol and defined concentration of

murine GM-CSF (Peprotech #315-03). For inhibitor studies, 100nM PD0325901 (Selleck Chemicals) solubilized in DMSO was added to methylcellulose media.

Tissue Histology

Tissue samples were fixed in 4% PFA, dehydrated with ethanol, cleared with xylenes and embedded in paraffin. 5um sections were cut on a rotary microtome and stained with hematoxylin and eosin.

Supplementary Figures

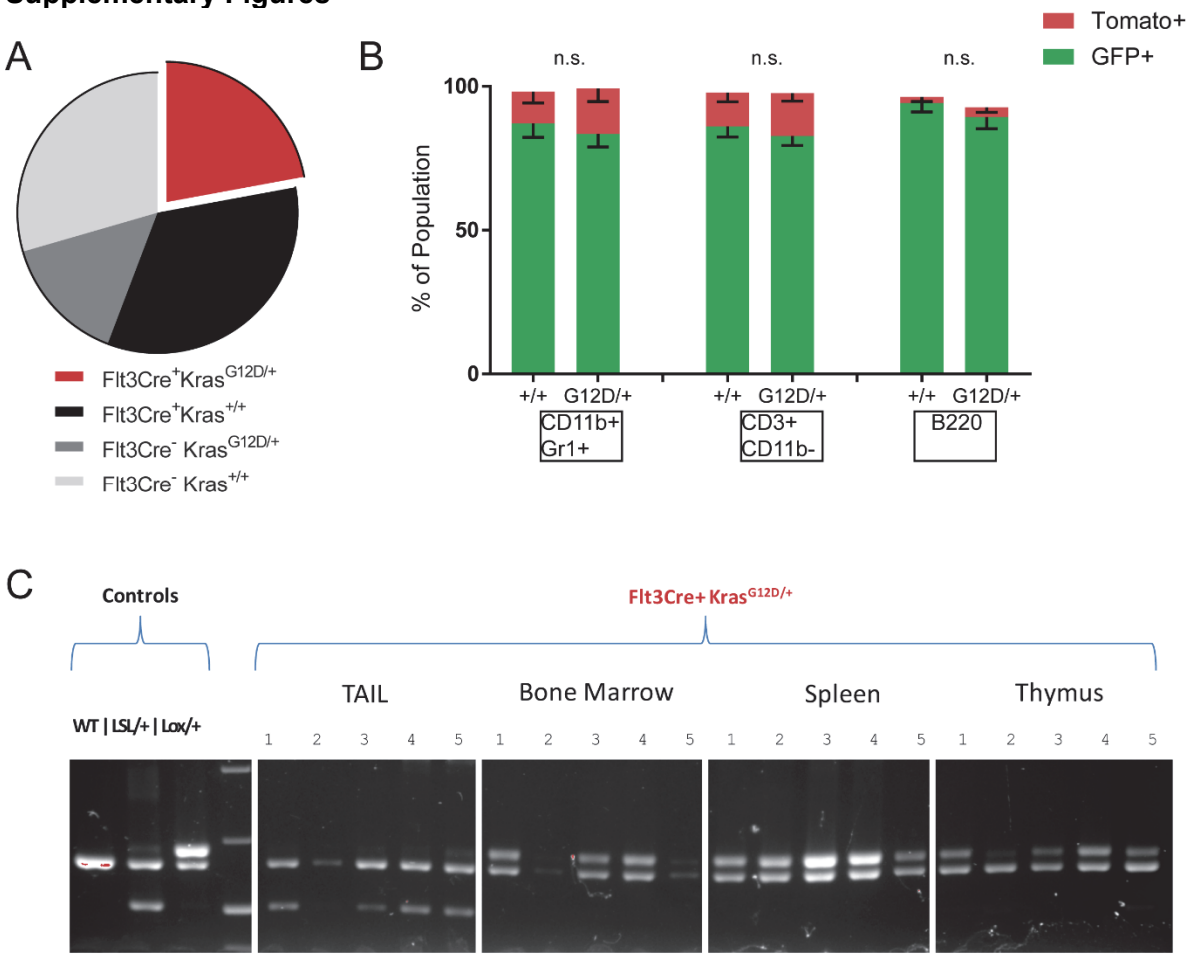

Figure S1. Flt3Cre+;Kras^{G12D} are born at expected Mendelian frequency, have equivalent Cre efficiency to controls, and have recombined the LSL-Kras^{G12D} locus. A) Genotypes at birth of Flt3Cre+ ROSA26$^{mTmG/mTmG}$ x LSL-Kras$^{G12D/+}$ progeny (N=95, Chi squared p=0.05). B) Proportion of peripheral blood cell lineages that express Tomato or GFP in mutant animals (N=10) and littermates (N=8). Statistical analysis by two-way ANOVA followed by Tukey's multiple comparisons test. C) PCR gel electrophoresis demonstrating successful recombination of the Lox-STOP-Lox Kras^{G12D} allele in the bone marrow, spleen, and thymus of 5 analyzed Flt3Cre+;Kras^{G12D} animals.

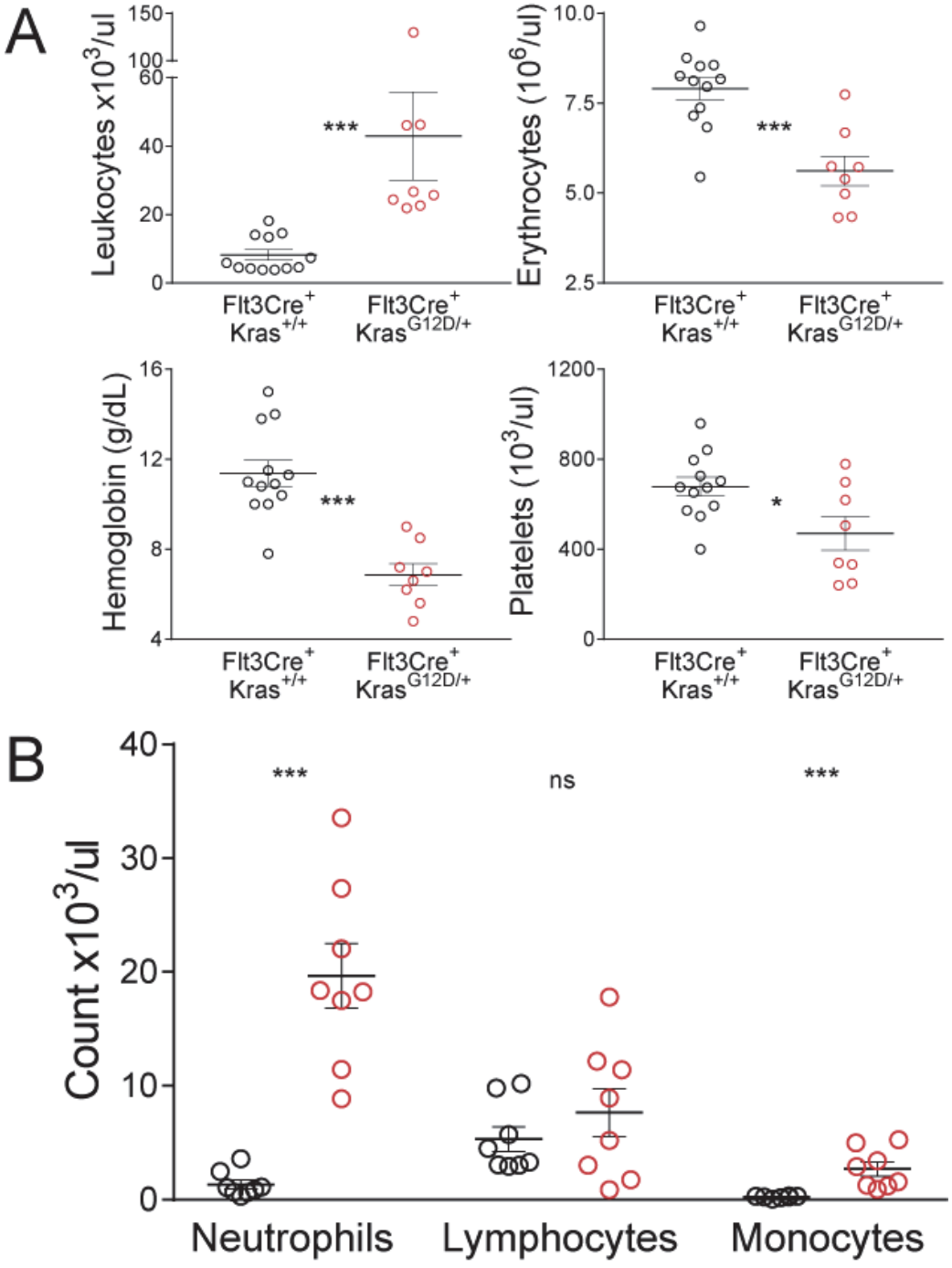

Figure S2. Flt3Cre+;Kras^{G12D} CBC analysis. Related to Figure 1C. A) Leukocyte, erythrocyte, and platelet counts and hemoglobin values in moribund mutant mice and littermate controls. B) Neutrophil, lymphocyte, and monocyte counts in moribund mutants and age-matched littermates as measured by a hematology analyzer.

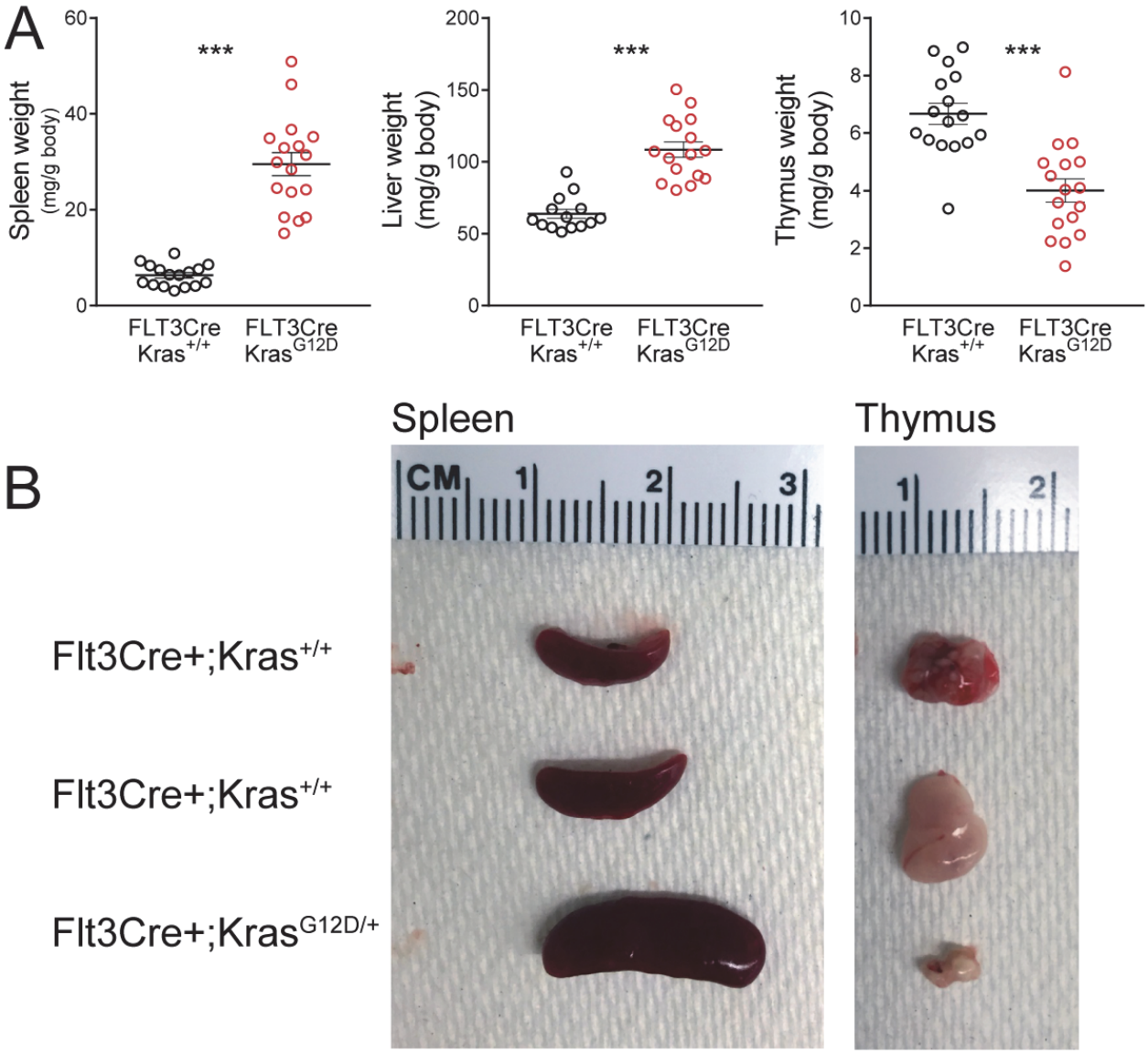

Figure S3. Hepatosplenomegaly and thymus atrophy in Flt3Cre+;Kras^{G12D} mice. A) Spleen, liver, and thymus weights normalized to body weight. B) Representative images of spleen and thymus sizes of one moribund 4 week old Flt3Cre+;Kras^{G12D} in comparison to two Flt3Cre+;Kras$^{+/+}$ littermates.

Flt3Cre;Kras+/+ **Flt3Cre;KrasG12D**

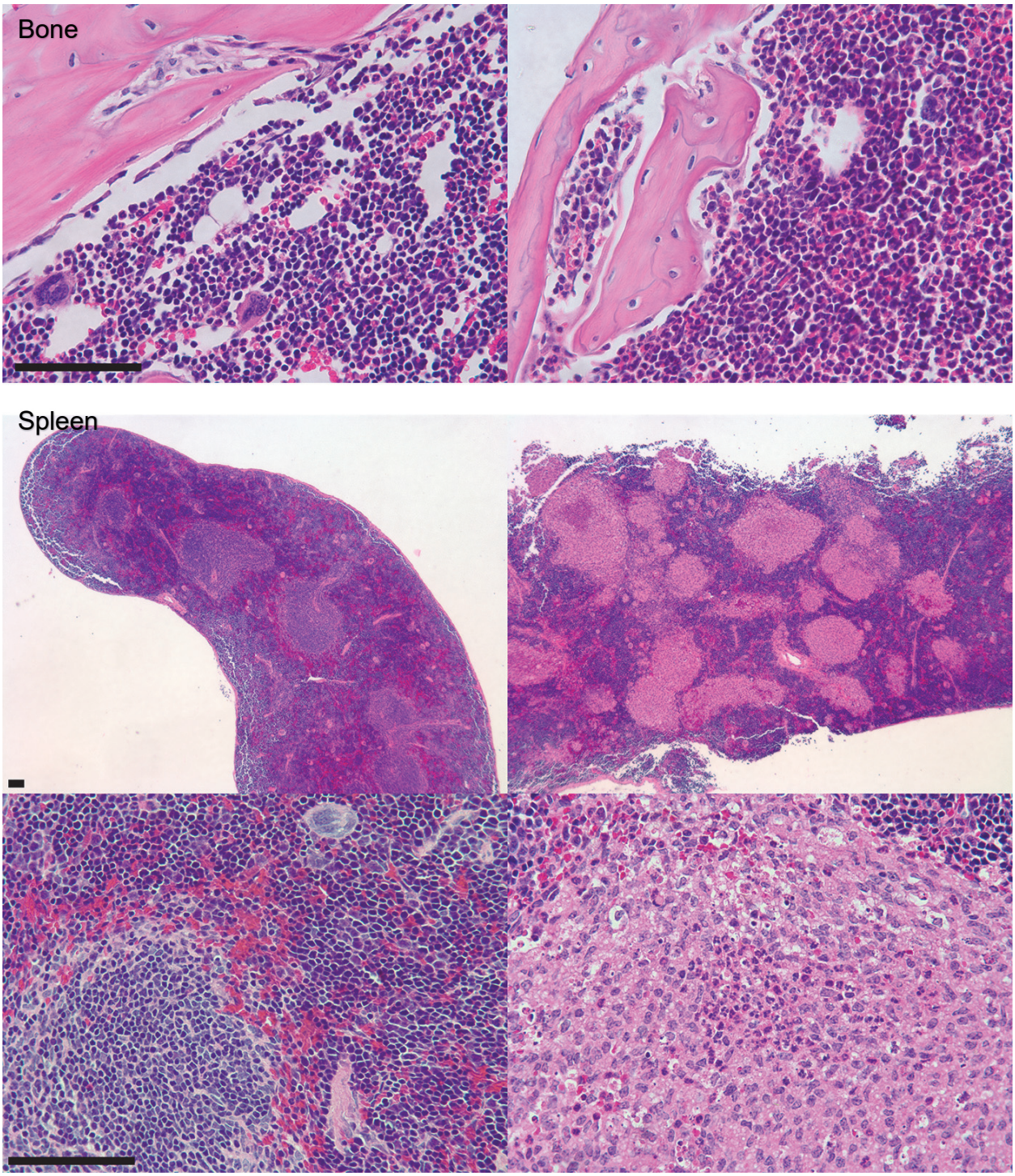

Figure S4A) Histology of bone and spleen from mutant animals and littermates.
Representative of N=2/group. Scale bars=100um.

Flt3Cre;Kras+/+ **Flt3Cre;KrasG12D**

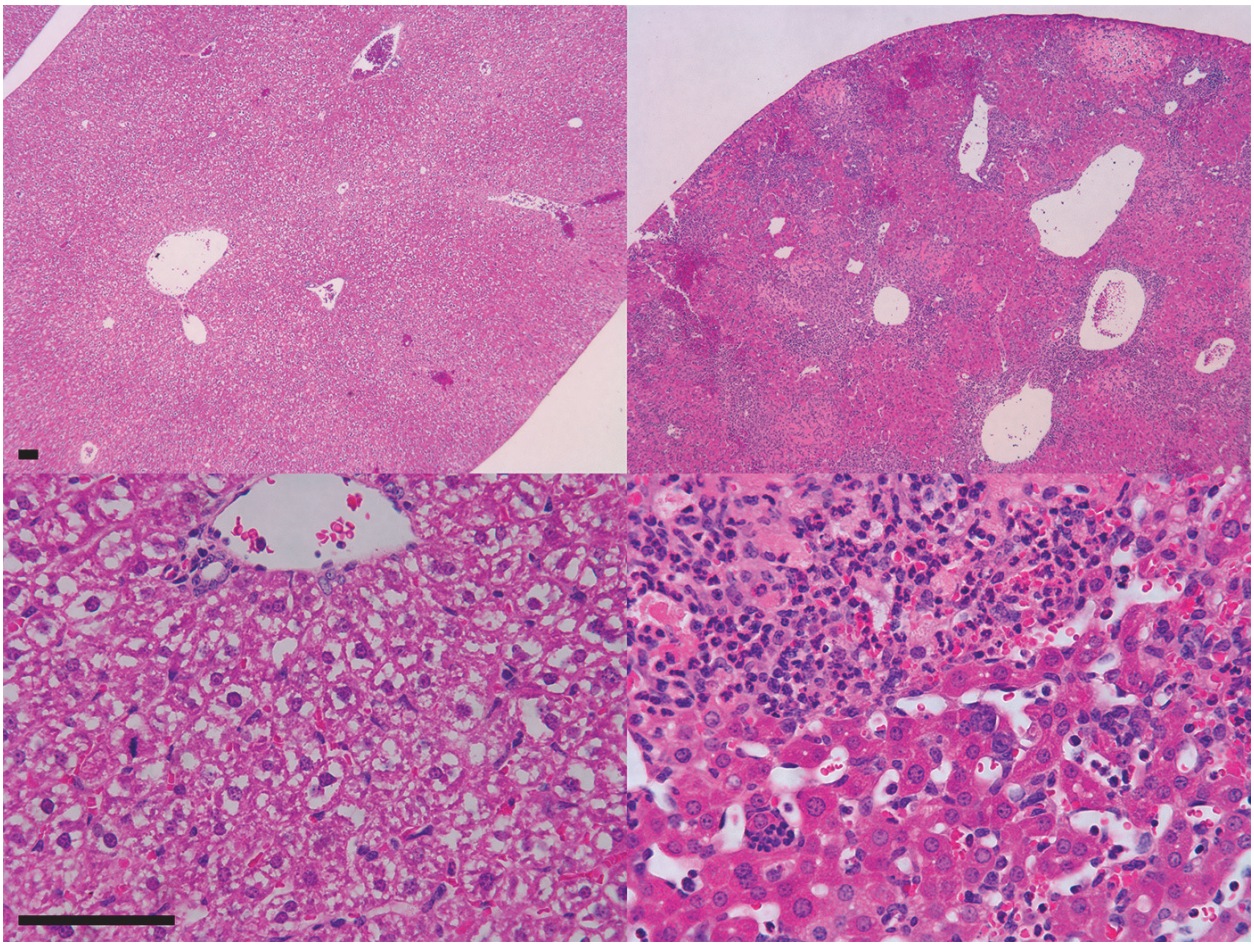

Figure S4B) Histology of liver from mutant animals and littermates. Representative of N=2/group. Scale bars=100um.

Flt3Cre;Kras+/+ **Flt3Cre;KrasG12D**

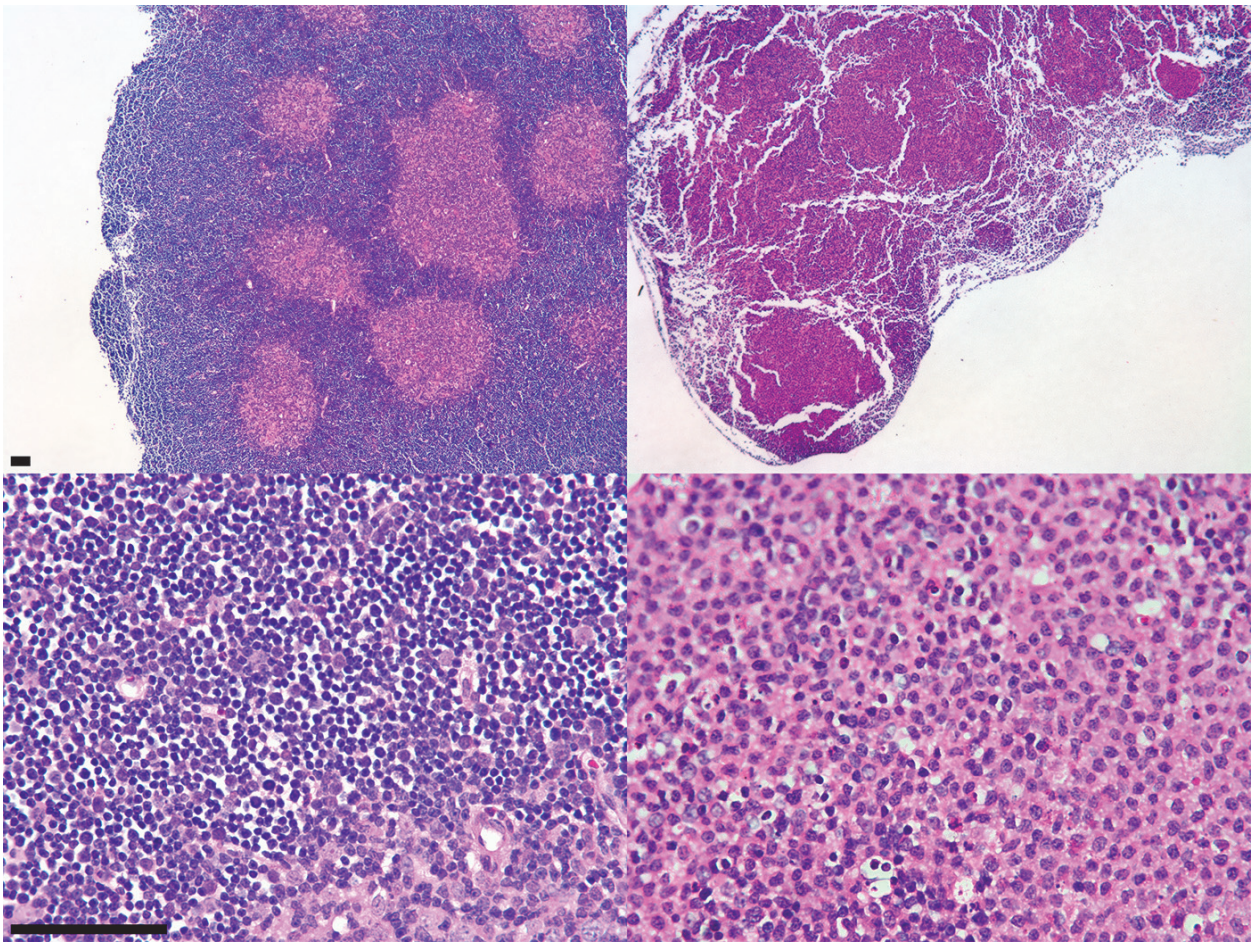

Figure S4C) Histology of thymus from mutant animals and littermates. Representative of N=2/group. Scale bars=100um.

Flt3Cre;Kras+/+ **Flt3Cre;KrasG12D**

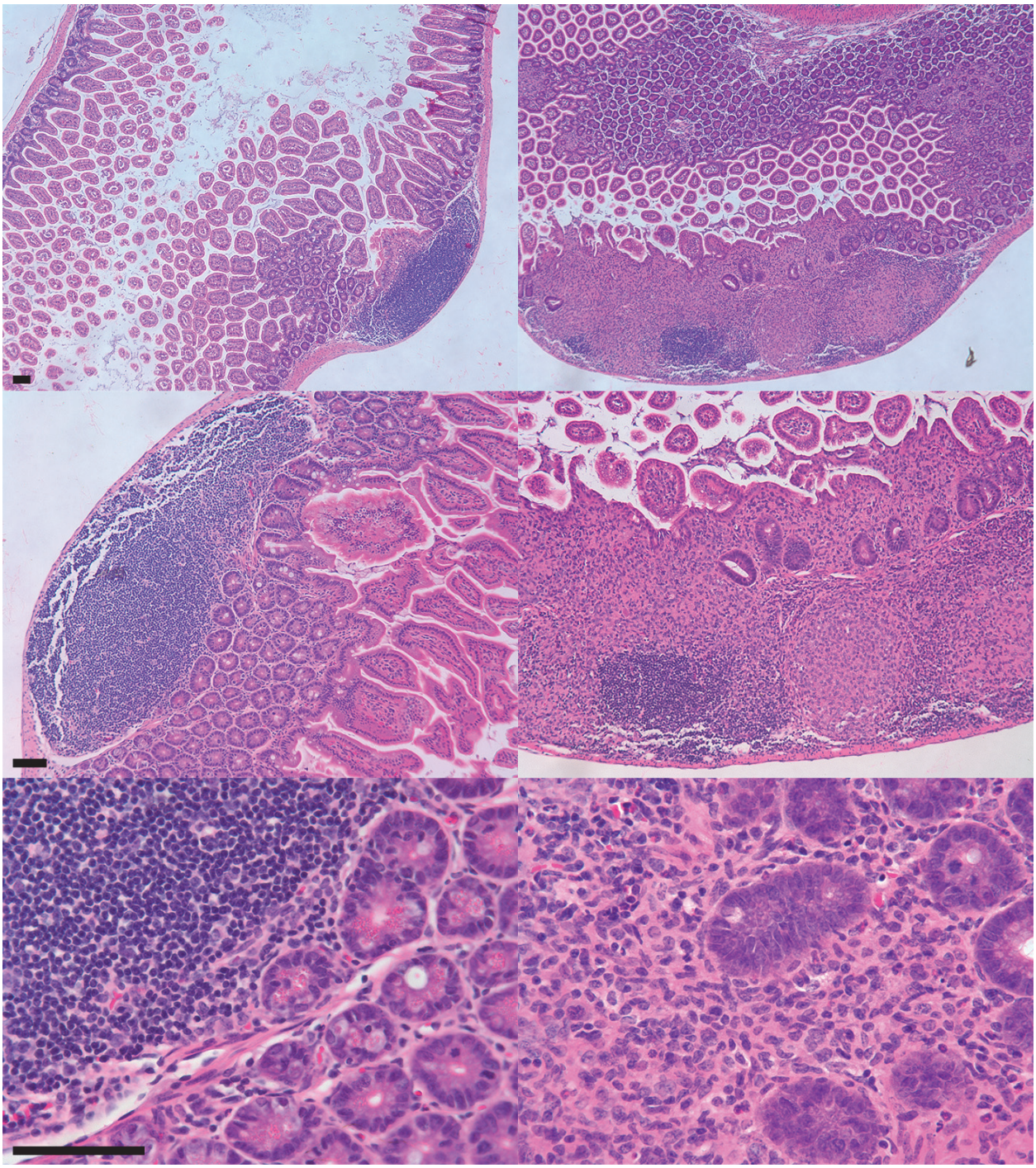

Figure S4D) Histology of GI from mutant animals and littermates. Representative of N=2/group. Scale bars=100um.

Flt3Cre;Kras+/+ **Flt3Cre;KrasG12D**

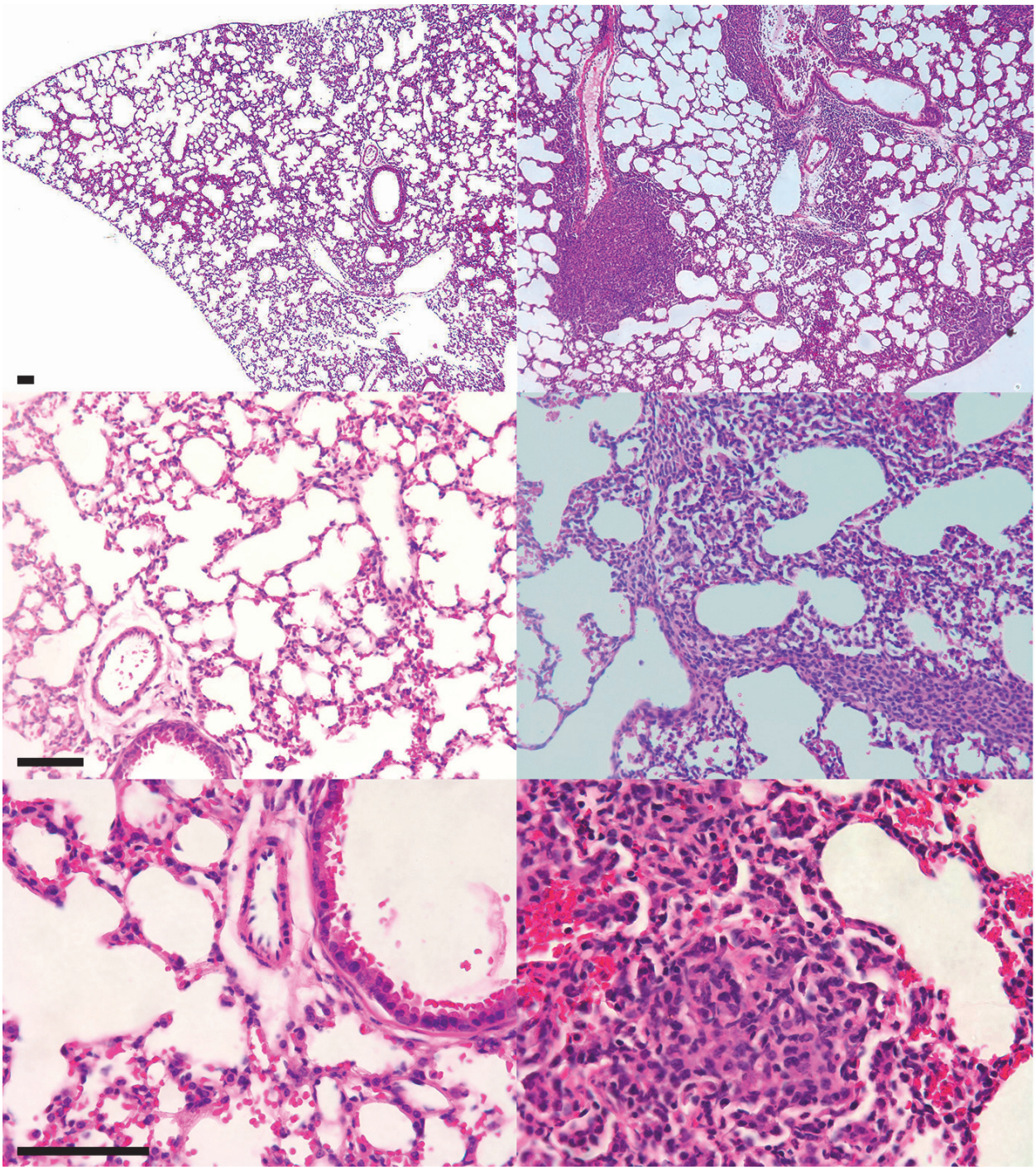

Figure S4E) Histology of lung from mutant animals and littermates. Representative of N=2/group. Scale bars=100um.

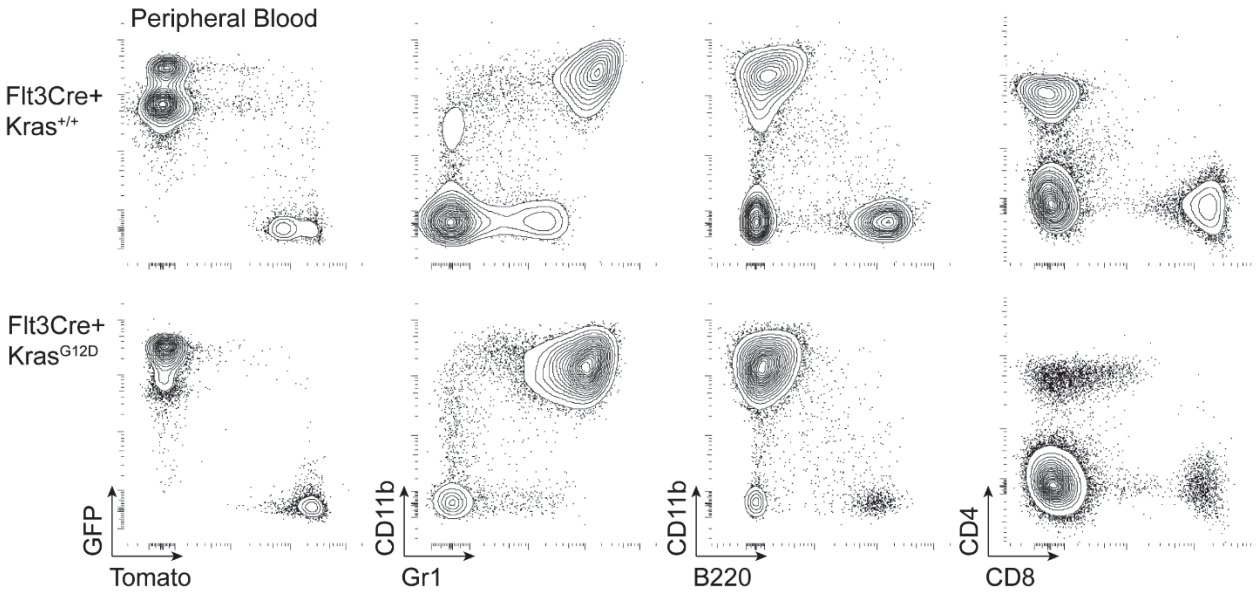

Figure S5. Representative peripheral blood flow cytometry of Flt3Cre+;Kras^{G12D} moribund mice and littermate controls. CD11b+ Gr1+ neutrophils are massively expanded in mutants with a concomitant decrease of B cells and T cells. In contrast to moribund Mx1Cre+;Kras^{G12D} mice, no evidence of CD4+ CD8+ double positive T cells are observed. Related to Figure 1E.

A

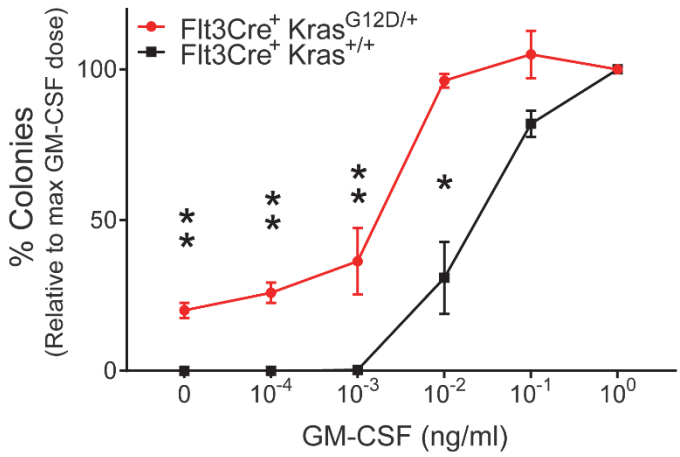

B

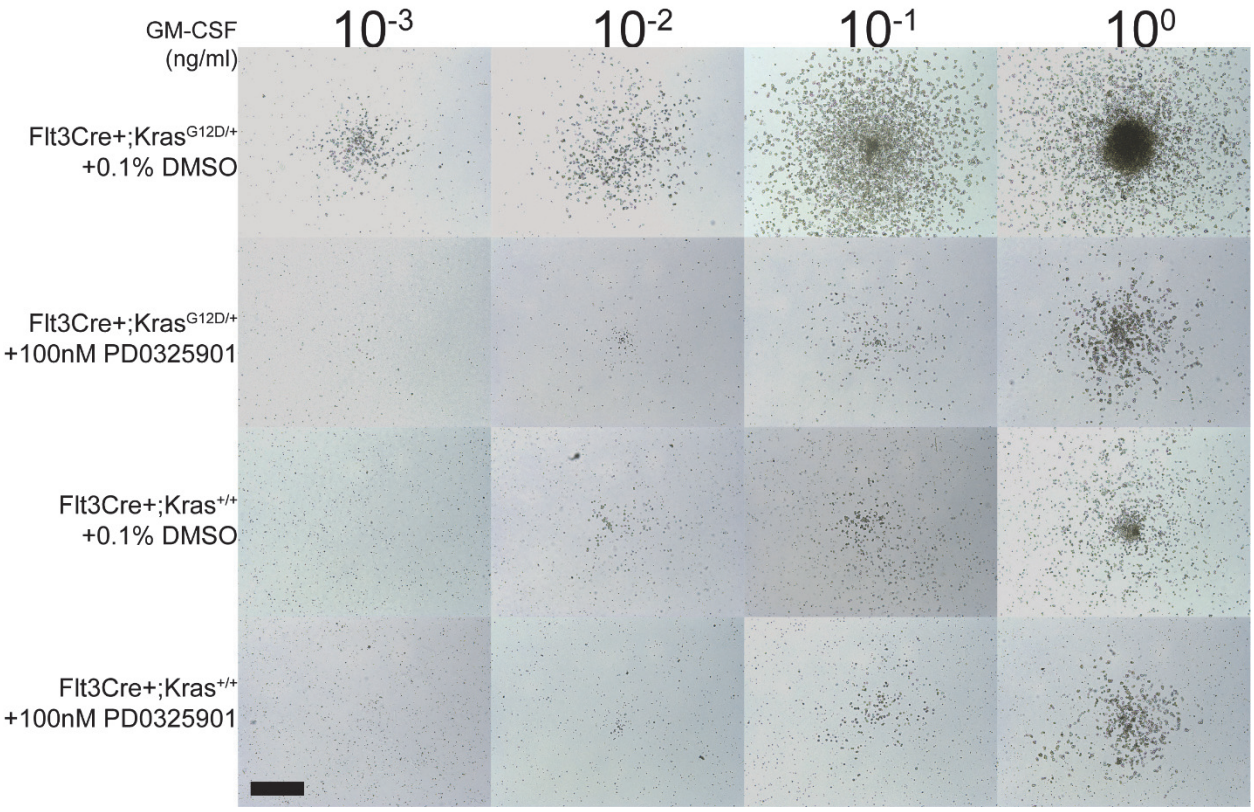

Figure S6. GM-CSF Hypersensitivity in Flt3Cre+;Kras^{G12D} mice is abrogated by MEK inhibition. A) 7 day methylcellulose colony formation of BM cells (N=2 mutant and 3 littermate biological replicates) B) Representative images of colonies are shown in Figure 1F. BM cells from Flt3Cre+;Kras^{G12D} mice or littermates were plated in methylcellulose medium with specified concentrations of GM-CSF and 100nM PD0325901 or DMSO vehicle control (N=3 animals/group; plated in triplicate). Scale bar = 0.5mm.

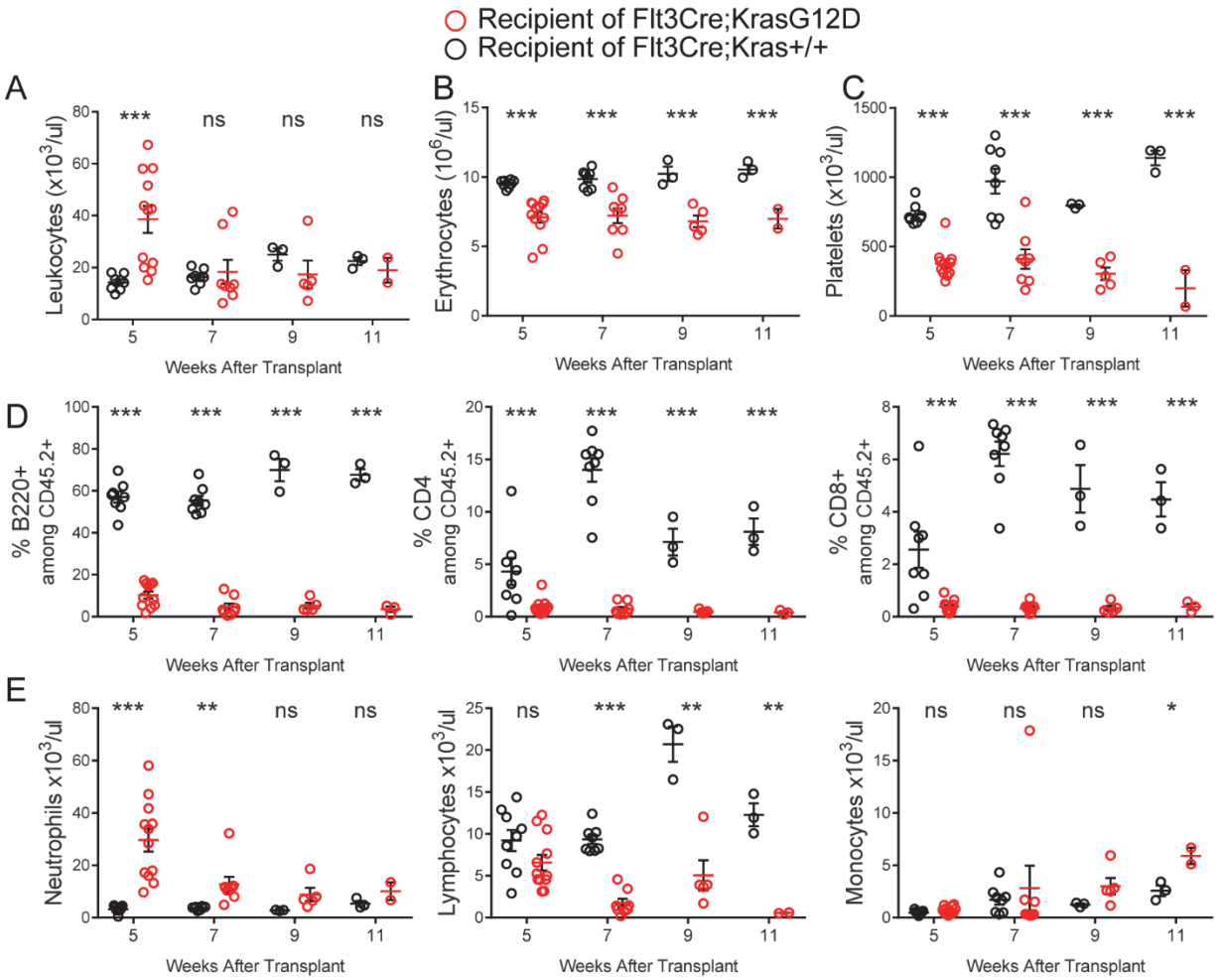

Figure S7. Peripheral blood analysis of adult BoyJ animals transplanted with E14.5 fetal liver cells from Flt3Cre+;Kras^{G12D} embryos or littermates. Related to Figure 2. A-C) Total leukocyte, erythrocyte, and platelet counts. D) Flow cytometric analysis of donor-derived B220+ B cell and CD4+ and CD8+ T cells in peripheral blood. Related to Figure 2C. E) Absolute neutrophil, lymphocyte, and monocyte counts. P values were calculated using two tailed t tests.

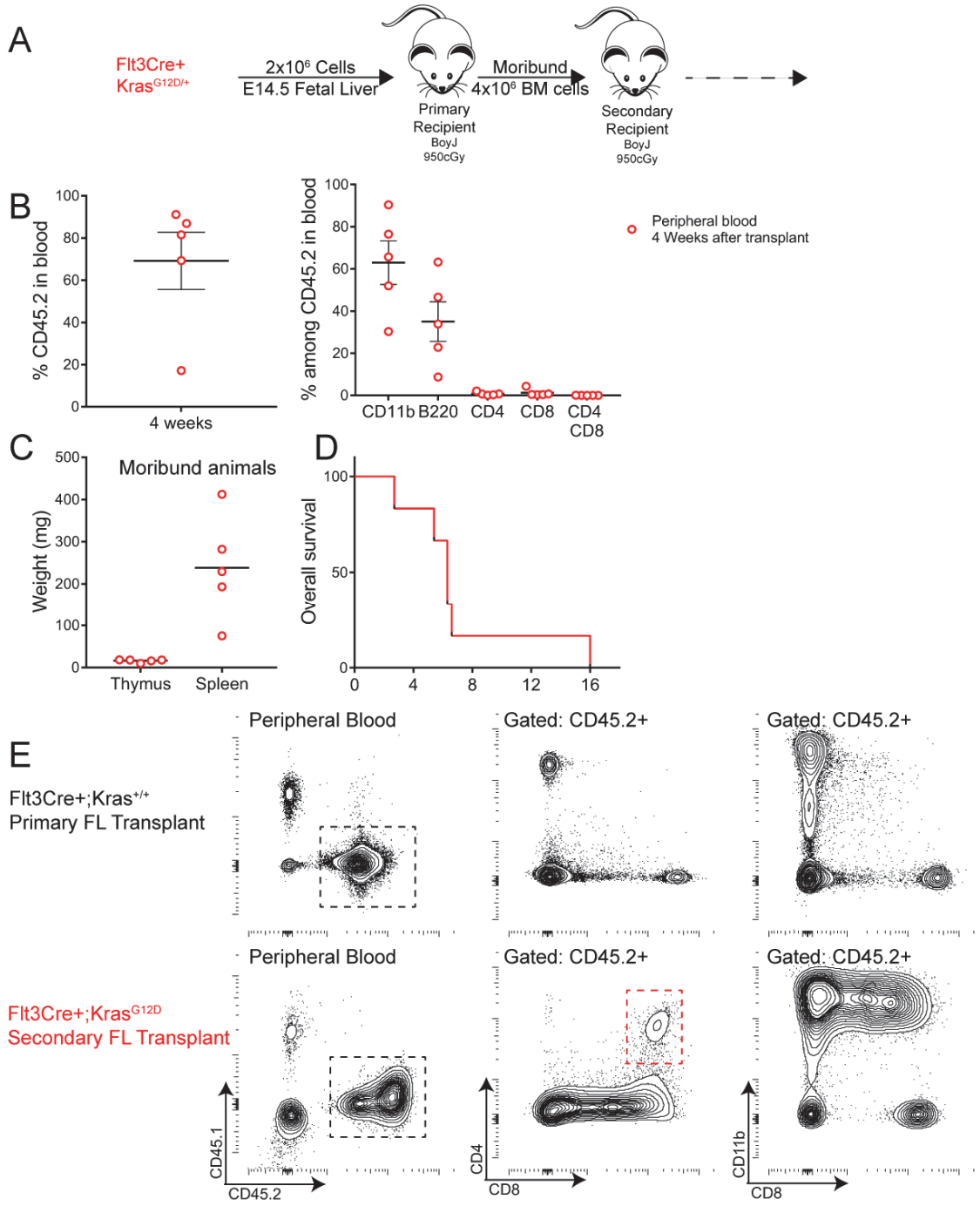

Figure S8. Analysis of Flt3Cre+;Kras^{G12D} secondary transplants. A) 4x10^6 BM cells from moribund primary recipients of Flt3Cre+;Kras^{G12D} E14.5 FL cells were secondarily transplanted into lethally irradiated BoyJ recipients. B) Peripheral blood analysis 4 weeks after transplant. C) Thymus and spleen weights of moribund secondary recipients. D) Overall survival. E) The longest surviving secondary recipient (16 weeks post-transplant) showed CD45.2+ CD4+ CD8+ double positive T-cells in peripheral blood when moribund, suggesting emerging T-ALL. Nevertheless, the animal succumbed with a small thymus (19mg) and the majority of peripheral leukocytes were CD11b+. The control primary FL transplant sample was analyzed concurrently and is shown as gating control.

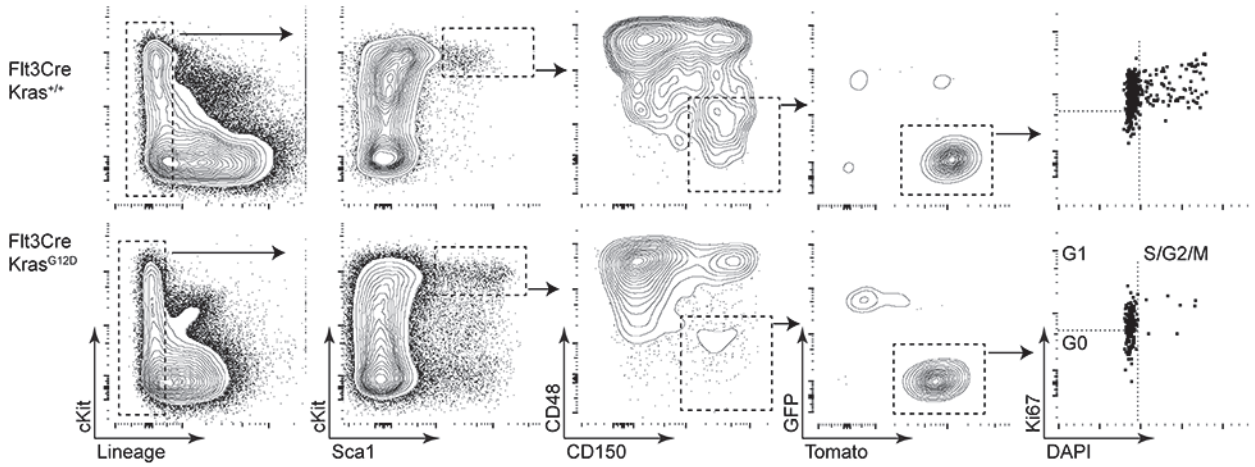

Figure S9. Cell cycle gating of Tomato+ HSCs in Flt3Cre+;Kras^{G12D}. Representative image of mutant and WT liver samples from 1 day-old littermates. Related to Figure 3B.

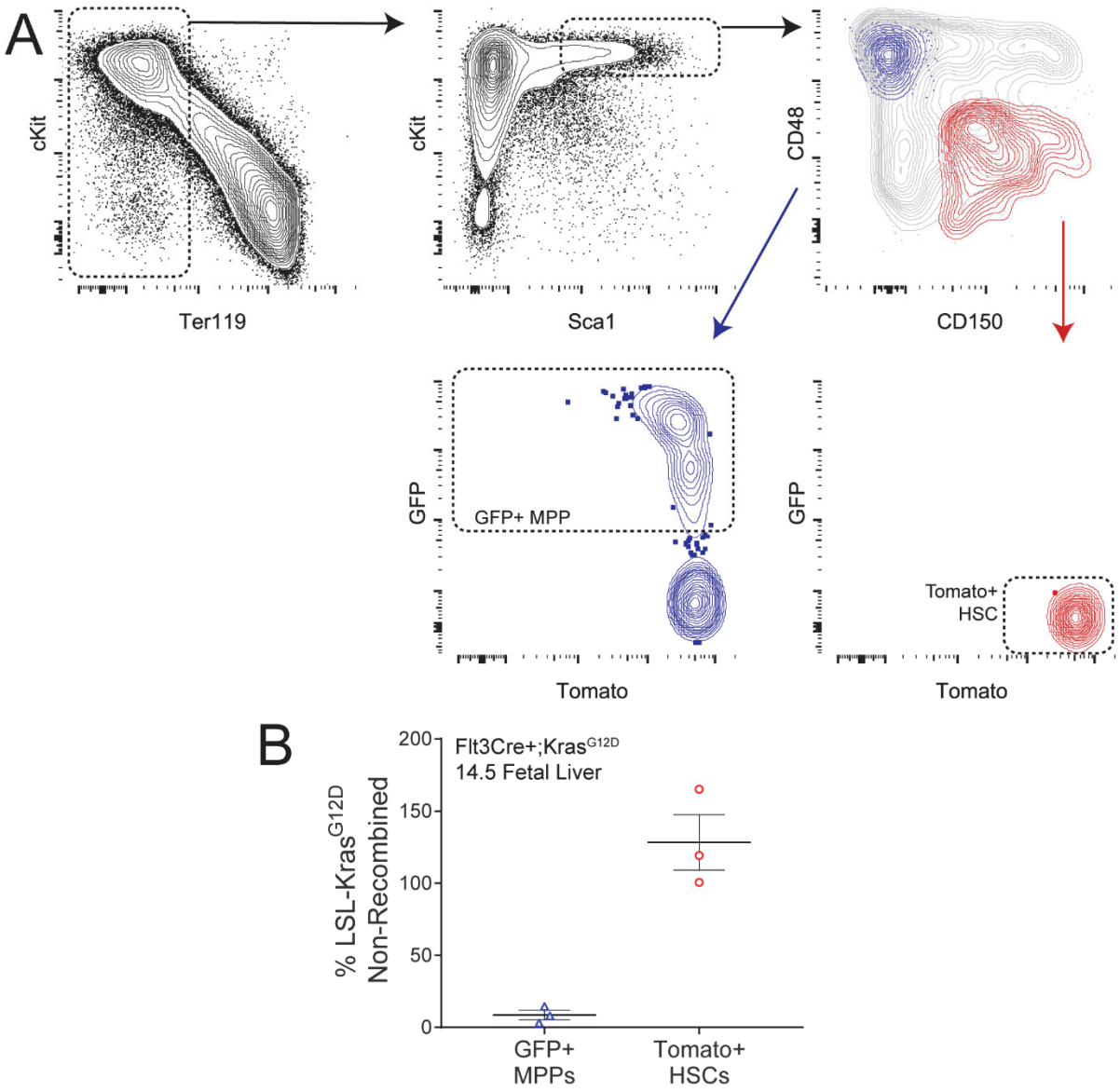

Figure S10. Fetal liver HSCs do not express the Cre recombinase in Flt3Cre+;Kras^{G12D} embryos. A) Representative gating of E14.5 FLT3Cre;Kras^{G12D} fetal liver cells. In red are shown phenotypic HSCs. In blue are shown phenotypic MPPs. GFP expression is only observed in the MPP compartment. HSCs remain Tomato+. B) Genomic DNA was isolated from sorted GFP+ MPPs and Tomato+ HSCs and subjected to qPCR to measure the abundance of the STOP cassette in the LSL-Kras^{G12D} locus.

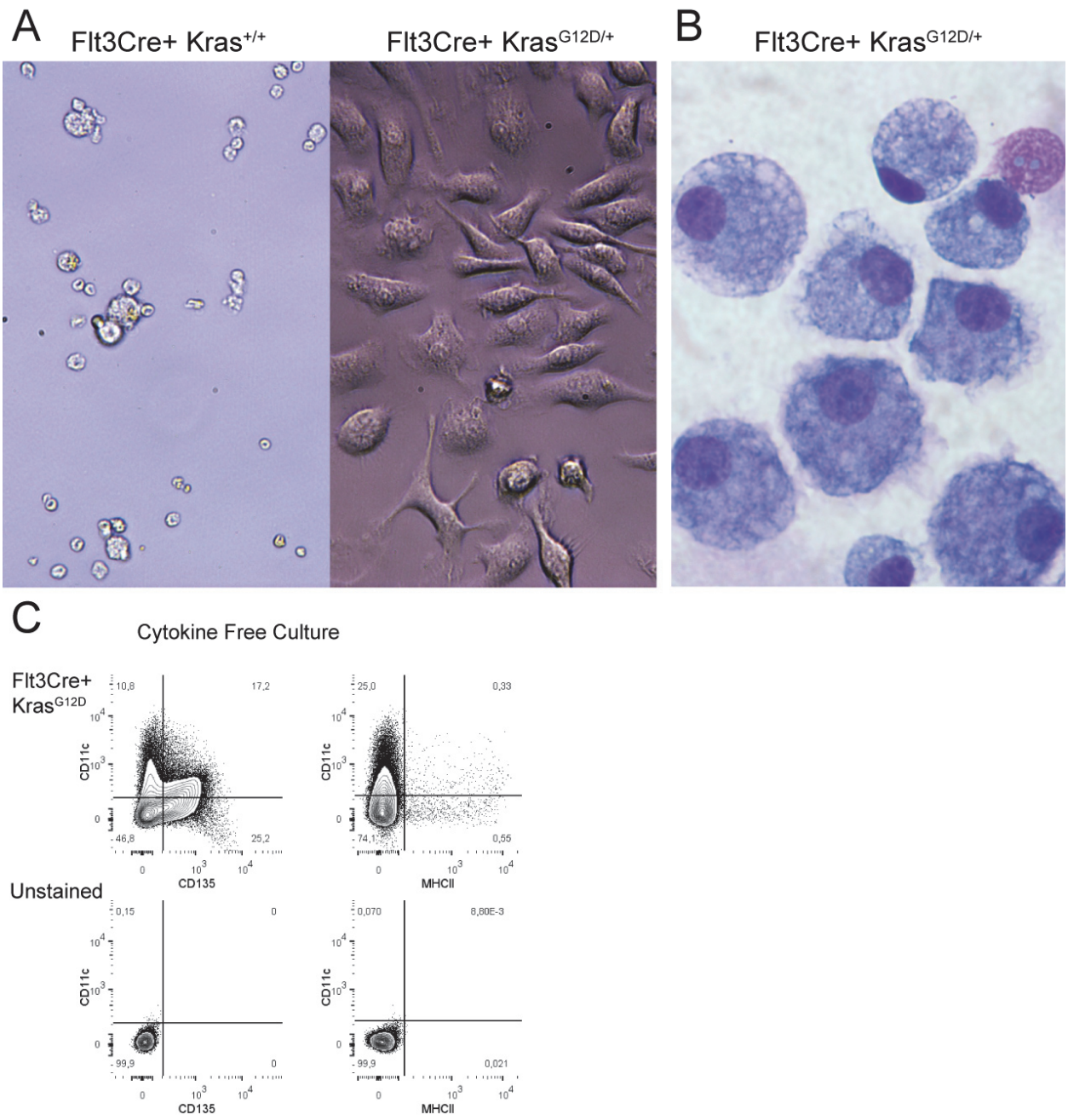

Figure S11. BM cells from Flt3Cre+;Kras^{G12D} spontaneously differentiate into dendritic cell-like cells. A) Phase contrast images of 7 day cytokine-free cultures of BM cells isolated from Flt3Cre+;Kras^{G12D} animals and healthy littermates (representative of N=4/group). B) Modified Wright stained cell cytospins of Flt3Cre+;Kras^{G12D} cultures shown in panel A (representative of N=2). C) Immunophenotype of cytokine-free Flt3Cre+;Kras^{G12D} BM cultures.

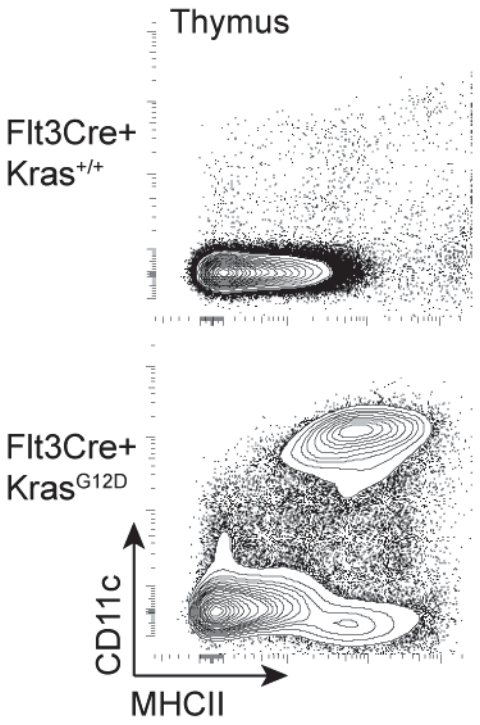

Figure S12. Representative gating of thymic dendritic cells in Flt3Cre+;Kras^{G12D} mice and littermate controls. Related to Figure 3C.

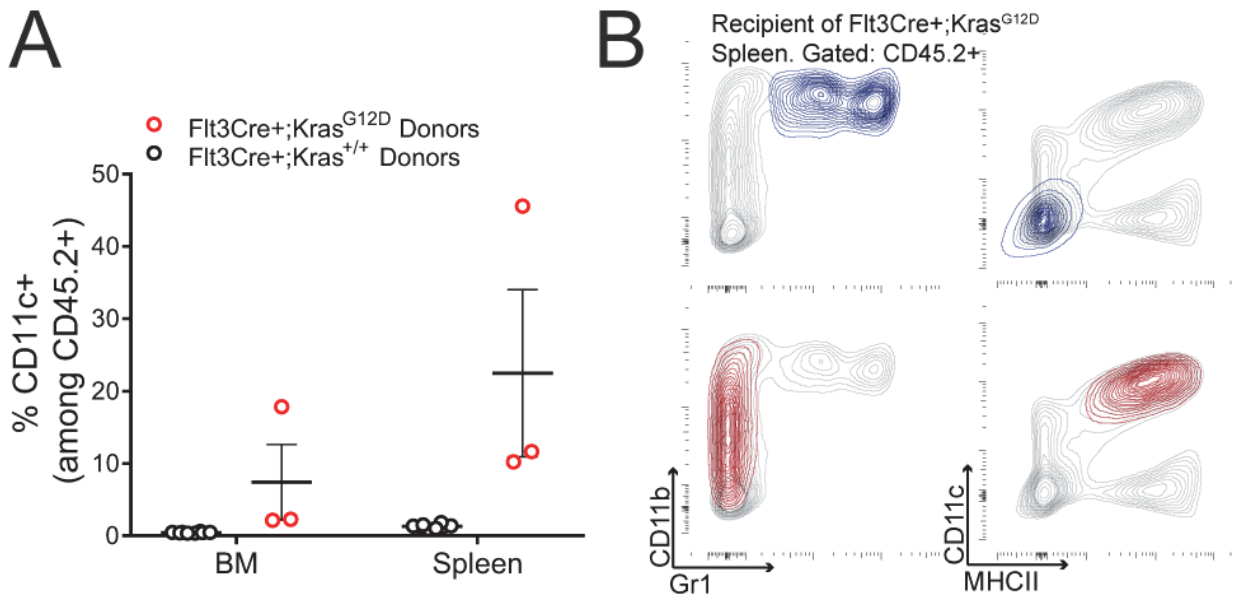

Figure S13. Dendritic cell expansion in BoyJ recipients of E14.5 Flt3Cre+;Kras^{G12D} fetal liver cells. A) Donor-derived CD11c+ cell frequency in recipients of FL progenitors. B) Representative gating of splenic engraftment in one BoyJ recipient following Flt3Cre+;Kras^{G12D} FL transplant. CD11c+ MHCII+ dendritic cells (red) are distinct from CD11b+ Gr1+ neutrophils (blue). Related to Figure 2.

Manufacturer	Catalog number	Antibody	Clone
eBioscience	45-0454-82	Anti-MouseCD45.2PerCP-Cyanine5.5	104
BioLegend	109830	PE/Cy7anti-mouseCD45.2vAntibody	104
BioLegend	109814	APCanti-mouseCD45.2 Antibody	104
BDBiosciences	51-01082J	Biotin Hamster anti-MouseCD3e	145-2C11
eBioscience	17-0031-82	Anti-MouseCD3eAPC	145-2C11
BioLegend	100334	PacificBlue™anti-mouseCD3ε Antibody	145-2C11
eBioscience	47-1171-82	Anti-MouseCD117(c-Kit)APC-eFluor®780	2B8
BioLegend	105814	PE/Cy7anti-mouseCD117(c-Kit) Antibody	2B8
BioLegend	140416	PE/Cy7anti-mouseCD8b.2 Antibody	53-5.8
Biolegend	100704	Biotinanti-mouseCD8a Antibody	53-6.7
Biolegend	100712	APCanti-mouseCD8a Antibody	53-6.7
eBioscience	47-0453-82	Anti-MouseCD45.1APC-eFluor®780	A20
BioLegend	135307	Biotinanti-mouseCD135 Antibody	A2F10
eBioscience	46-1351-82	Anti-MouseCD135(Flt3)PerCP-eFluor®710	A2F10
Biolegend	108128	BrilliantViolet421™anti-mouseLy-6A/E(Sca-1) Antibody	D7
Biolegend	108141	AlexaFluor®700anti-mouseLy-6A/E	D7
Biolegend	100404	Biotinanti-mouseCD4Antibody	GK1.5
Biolegend	100443	BrilliantViolet421™anti-mouseCD4 Antibody	GK1.5
Biolegend	100413	APC/Cy7anti-mouseCD4 Antibody	GK1.5
Biolegend	103432	APC/Cy7anti-mouseCD48 Antibody	HM48-1
BDBiosciences	51-01712J	BiotinRatanti-MouseCD11b	M1/70
Biolegend	101224	PacificBlue™anti-mouse/humanCD11b Antibody	M1/70
BioLegend	101212	APCanti-mouse/humanCD11b Antibody	M1/70
Biolegend	107614	APCanti-mouseI-A/I-E Antibody	M5/114.15.2
Biolegend	117303	Biotinanti-mouseCD11c Antibody	N418
Biolegend	117323	APC/Cy7anti-mouseCD11c Antibody	N418
Biolegend	117328	PerCP/Cy5.5anti-mouseCD11c Antibody	N418
Biolegend	102029	PerCP/Cy5.5anti-mouseCD25 Antibody	PC61
BDBiosciences	51-01122J	BiotinRatanti-MouseCD45R	RA3-6B2
eBioscience	25-0452-82	Anti-Human/MouseCD45R(B220)PE-Cyanine7	RA3-6B2
eBioscience	47-0452-82	Anti-Human/MouseCD45R(B220)APC-eFluor®780	RA3-6B2
BDBiosciences	51-01212J	BiotinRatanti-MouseLy-6GandLy-6C	RB6-8C5
Biolegend	108427	PerCP/Cy5.5anti-mouseLy-6G/Ly-6C(Gr-1) Antibody	RB6-8C5
Biolegend	115910	APCanti-mouseCD150(SLAM) Antibody	TC15-12F12.2
BDBiosciences	51-09082J	BiotinRatanti-MouseTER-119/Erythroid cells	TER-119
Biolegend	405229	BrilliantViolet605™Streptavidin	
Biolegend	405214	PerCP/Cy5.5Streptavidin	
Biolegend	405241	BrilliantViolet711™Streptavidin	
BDBiosciences	551487	PE-Texas Red Streptavidin	
Biolegend	652423	PerCP/Cy5.5 anti-mouse Ki-67 Antibody	16A8
Biolegend	423103	ZombieYellow™FixableViabilityKit	

Table 1. List of antibodies.

Reaction	Primers	Interpretation
LSL-KrasG12D Genotyping	GTCTTTCCCCAGCACAGTGC	WT Kras Allele=622bp
	CTCTTGCCTACGCCACCAGCTC	LSL-KrasG12D=500bp
	AGCTAGCCACCATGGCTTGAGTAAGTCTGCA	loxP-KrasG12D=650bp
Sly / Xlr (gender) Genotyping (6)	GATGATTTGAGTGGAAATGTGAGGTA	Male=280bp
	CTTATGTTTATAGGCATGCACCATGTA	Female=480bp+660bp+685bp
LSL-KrasG12D Recombination Genomic DNA qPCR	CTAGCCACCATGGCTTGAGT	
	GCAGCTAATGGCTCTCAAAGGA	
Murine SRY Genomic DNA qPCR (7)	CTCATCGGAGGGCTAAAGTG	
	AAGCTTTGCTGGTTTTTGGA	

Table 2. List of primers used for genotyping and qPCR.

Supplemental References

1. Braun BS, Tuveson DA, Kong N, Le DT, Kogan SC, Rozmus J, et al. Somatic activation of oncogenic Kras in hematopoietic cells initiates a rapidly fatal myeloproliferative disorder. *Proc Natl Acad Sci USA.* 2004;101(2):597-602.
2. Muzumdar MD, Tasic B, Miyamichi K, Li L, and Luo L. A global double-fluorescent Cre reporter mouse. *Genesis.* 2007;45(9):593-605.
3. Epelman S, Lavine KJ, Beaudin AE, Sojka DK, Carrero JA, Calderon B, et al. Embryonic and adult-derived resident cardiac macrophages are maintained through distinct mechanisms at steady state and during inflammation. *Immunity.* 2014;40(1):91-104.
4. Benz C, Martins VC, Radtke F, and Bleul CC. The stream of precursors that colonizes the thymus proceeds selectively through the early T lineage precursor stage of T cell development. *The Journal of experimental medicine.* 2008;205(5):1187-99.
5. Nabinger SC, Li XJ, Ramdas B, He Y, Zhang X, Zeng L, et al. The protein tyrosine phosphatase, Shp2, positively contributes to FLT3-ITD-induced hematopoietic progenitor hyperproliferation and malignant disease in vivo. *Leukemia.* 2013;27(2):398-408.
6. McFarlane L, Truong V, Palmer JS, and Wilhelm D. Novel PCR assay for determining the genetic sex of mice. *Sexual development : genetics, molecular biology, evolution, endocrinology, embryology, and pathology of sex determination and differentiation.* 2013;7(4):207-11.
7. D'Hulst C, Parvanova I, Tomoiaga D, Sapar ML, and Feinstein P. Fast quantitative real-time PCR-based screening for common chromosomal aneuploidies in mouse embryonic stem cells. *Stem cell reports.* 2013;1(4):350-9.